



Seismic and acoustic recordings of an unusually large rockfall at Mount St. Helens, Washington

S. C. Moran,¹ R. S. Matoza,² M. A. Garcés,³ M. A. H. Hedlin,² D. Bowers,⁴ W. E. Scott,¹ D. R. Sherrod,¹ and J. W. Vallance¹

Received 30 June 2008; revised 26 August 2008; accepted 28 August 2008; published 2 October 2008.

[1] On 29 May 2006 a large rockfall off the Mount St. Helens lava dome produced an atmospheric plume that was reported by airplane pilots to have risen to 6,000 m above sea level and interpreted to be a result of an explosive event. However, subsequent field reconnaissance found no evidence of a ballistic field, indicating that there was no explosive component. The rockfall produced complex seismic and infrasonic signals, with the latter recorded at sites 0.6 and 13.4 km from the source. An unusual, very long-period (50 s) infrasonic signal was recorded, a signal we model as the result of air displacement. Two high-frequency infrasonic signals are inferred to result from the initial contact of a rock slab with the ground and from interaction of displaced air with a depression at the base of the active lava dome. **Citation:** Moran, S. C., R. S. Matoza, M. A. Garcés, M. A. H. Hedlin, D. Bowers, W. E. Scott, D. R. Sherrod, and J. W. Vallance (2008), Seismic and acoustic recordings of an unusually large rockfall at Mount St. Helens, Washington, *Geophys. Res. Lett.*, 35, L19302, doi:10.1029/2008GL035176.

1. Introduction

[2] In 2004 Mount St. Helens (MSH) began erupting continuously after an 18-year hiatus [Dzurisin *et al.*, 2005]. Shortly after the eruption began, collocated acoustic and seismic instruments were installed at two sites to enable detection of eruption-related acoustic signals (Figure 1). The first site (SEP), ~0.4 km from the vent, had a Mark Products L22 short-period three-component seismometer operated with high- and low-gain channels to increase dynamic range, and two short-period electret acoustic sensors separated by ~18 m [McChesney *et al.*, 2008] (any use of trade names is for descriptive purposes only and does not imply endorsement by the federal government). Data from this site were sent in real-time to the Cascades Volcano Observatory (CVO) and the Pacific Northwest Seismic Network (PNSN). The second site (CDWR), 13.4 km from the vent, had a Guralp CMG-40T broadband seismometer and a four-element array of MB2000 DASE/Tekelec broadband aneroid microbarometers arranged in a triangle with an

aperture of ~100 m [Matoza *et al.*, 2007]. Data from this site was sent via VSAT to a downlink station in Ottawa, Canada, and then to the University of California, San Diego, for analysis and archiving. Recordings and analysis of other signals recorded by these sensors are discussed by Matoza *et al.* [2007] and Moran *et al.* [2008].

[3] Rockfalls have been one of the principal sources of infrasonic signals during the eruption, particularly those associated with larger earthquakes ($M_d > 3$). Several rockfalls were witnessed by scientists working in the crater, and the formation of dust-and-ash plumes resulting from rockfalls has been well documented with photographs and/or video recordings. Owing to the gas-poor nature of the erupted lava, such events have not led to classic block-and-ash flows such as those observed at Unzen (Japan), Soufriere Hills (Montserrat), and other volcanoes during dome-building eruptions. Nevertheless, in a number of instances rockfall-derived dust plumes have risen hundreds of meters above the crater rim and from afar have been mistaken for explosive events by aviators and the general public.

2. The 29 May 2006 Rockfall

[4] At 1608 UTC on 29 May 2006 a shallow earthquake (depth < 0.5 km) and M_d 3.1 magnitude occurred beneath the dome. Several minutes after the earthquake, CVO received pilot reports of an ash plume extending from the crater to a peak height of ~6 km above sea level (~4.1 km above the vent). Photographs taken by passengers on commercial jets flying near the volcano at the time show a gray cauliflower-shaped plume that, over several minutes, rose rapidly above the crater rim but remained perceptibly attached to the crater via a narrow plume to the crater floor. Although airborne observers interpreted the event as explosive in nature, CVO issued a statement reporting that “a large rockfall from the growing lava dome corresponded with a magnitude 3.1 earthquake, sending a flow of rock and dust from the new dome.” This interpretation was based on seismic signals characteristic of a rockfall and on experience with previous plumes generated by rockfalls at MSH.

[5] Associated with this event were complex, large-amplitude infrasonic signals recorded at stations SEP and CDWR (Figure 2). An initial set of infrasonic signals (peak amplitudes 4–6.2 Pa at SEP, 0.06–0.08 Pa at CDWR (high-pass filtered at 1 Hz to be more comparable to the 1 Hz microphones at SEP)) arrived 1.5 s after the initial seismic signal at SEP and 38 s later at CDWR, the expected time separations at both sites between *P*-waves and infrasonic waves originating from a near-vent source. A second,

¹Cascades Volcano Survey, U.S. Geological Survey, Vancouver, Washington, USA.

²Institute of Geophysics and Planetary Physics, Scripps Institution of Oceanography, University of California, San Diego, La Jolla, California, USA.

³Infrasound Laboratory, Hawai'i Institute of Geophysics and Planetology, University of Hawai'i at Manoa, Kailua-Kona, Hawai'i, USA.

⁴AWE Blacknest, Reading, UK.

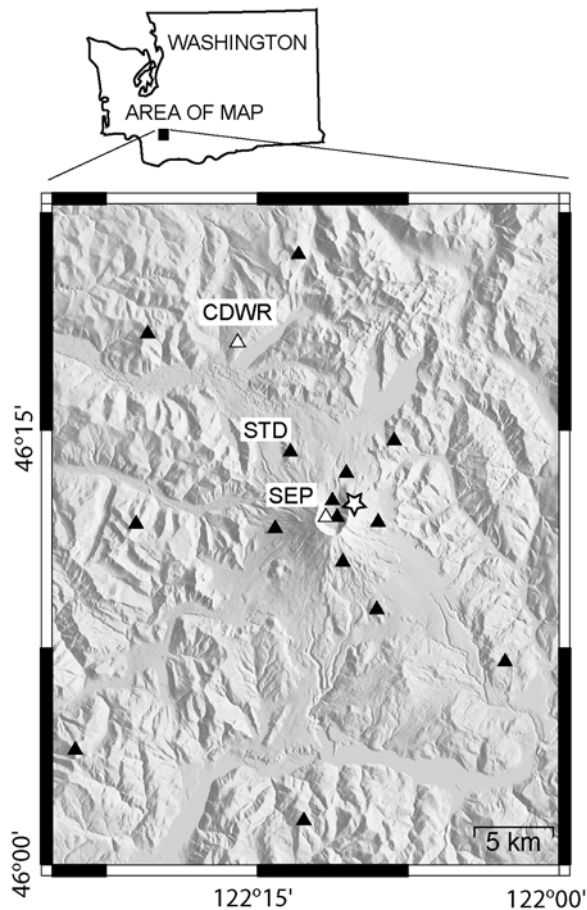


Figure 1. Shaded-relief map of Mount St. Helens and surrounding area, Washington. Black triangles represent seismic stations, white triangles indicate SEP and CDWR seismic/infrasound sites, and white star indicates location of remote camera that took Figure 3 pictures.

larger-amplitude infrasonic pulse (10.4–11 Pa at SEP, 0.25–0.3 Pa at CDWR) arrived ~ 15 s after the first. For simplicity we refer to the first set of infrasonic signals as A1 and the second as A2 (Figures 2b and 2e). Following A1 and continuing after A2, low-amplitude, high-frequency infrasonic signals were recorded at SEP and CDWR. These signals, which are temporally associated with low-amplitude, high-frequency seismic signals visible on the seismic channel of SEP (Figure 2a), are identical to those produced by many rockfalls recorded at MSH (i.e., broadband signals with teardrop- or spindle-shaped envelopes [e.g., Norris, 1994, Figure 2]).

[6] The peak amplitudes for A2 recorded at CDWR were equivalent to those from the 8 March 2005 explosive event at MSH [Matoza *et al.*, 2007], the largest of the 2004–2008 eruption. Unlike A1, no large-amplitude seismic signal was associated with A2 (Figures 2a and 2c). The acoustic/seismic amplitude ratios for A2 were much larger than for A1 at SEP and CDWR, indicating that the source for A2 was poorly coupled to the ground relative to A1. A search through recordings of previous large earthquakes at MSH between October 2004 and June 2007 revealed many instances of earthquakes with single infrasonic pulses sim-

ilar to A1 occurring within the first few seconds of the initial seismic waves, but no instances of secondary large-amplitude acoustic pulses.

[7] Accompanying the higher-frequency infrasonic signals was a ~ 50 -s-period, or very long-period (VLP), infrasonic pulse that can be seen in the raw and lowpass-filtered versions of the CDWR microbarometer records (Figures 2d and 2f). The onset of the VLP signal is coincident with the arrival of the A1 pulse, suggesting that it is related to the initial collapse of the rock mass. No time-correlative VLP signal was evident on records from the CDWR broadband seismometer or a PNSN/CVO broadband seismometer located 4 km northwest of the crater (STD, Figure 1). Subsequent analysis found several weaker VLP infrasonic pulses associated with other $M > 3$ earthquakes, but none with amplitudes as large as those of the 29 May 2006 VLP pulse. The VLP pulse was not observed at a similar acoustic array 250 km east of MSH near Kennewick, Washington.

3. Field Observations

[8] In the absence of field evidence, the 29 May 2006 rockfall might have been interpreted to be explosive given the above-average plume height and the large-amplitude infrasonic signals. However, clear weather at MSH allowed CVO geologists to make an aerial reconnaissance of the crater on 30 May 2006 and conduct a ground survey on 5 June 2006. They found a 1.3-km-long rockfall and mixed rock/snow avalanche deposit extending north from the extruding lava dome, over the east edge of the 1980–1986 lava dome, and terminating on the crater floor north of the 1980–1986 lava dome (Figure 3). The rockfall originated from the top of the active spine of the new lava dome (“spine 7” in Figure 3b), ~ 0.6 km from SEP and 13.6 km from CDWR, leaving behind a scar 50,000–100,000 m³ in volume (S. P. Schilling, USGS, personal communication, 2007). Substantial snow was scoured by and incorporated into the rockfall to form an avalanche of snow and rock debris that ran out across the thick snow pack covering the crater floor. The avalanche included hot boulders as large as 4 m in diameter that subsequently created deep melt pits. Thin ashfall deposits mantled the eastern arm of Crater Glacier adjacent to the rockfall, but there was no evidence of ballistic impact craters. In contrast, MSH explosive events in 2004 and 2005 sent ballistic projectiles hundreds of meters across the crater floor and created broad fields of small craters in snow-covered surfaces [Moran *et al.*, 2008].

[9] Other observations come from pictures of the steam plume (Figure 3) that were taken 6 and 66 minutes after the seismic event by a remote CVO camera located ~ 1 km from the vent on the east crater rim of MSH (white star in Figure 1). The pictures show that the plume originated in a depression 350 m from the rockfall source (Figures 3a and 3b). The depression was bounded by the growing lava dome to the south and west (“spines 3–5” and “spine 7” in Figure 3b), the 1980–1986 lava dome to the north, and the eastern arm of Crater Glacier to the east. Much of the rockfall debris was deposited in the depression. The depression was located ~ 0.25 km east of the vent that fed the 2004–2008 eruption. In summary, field evidence demonstrated that the 29 May

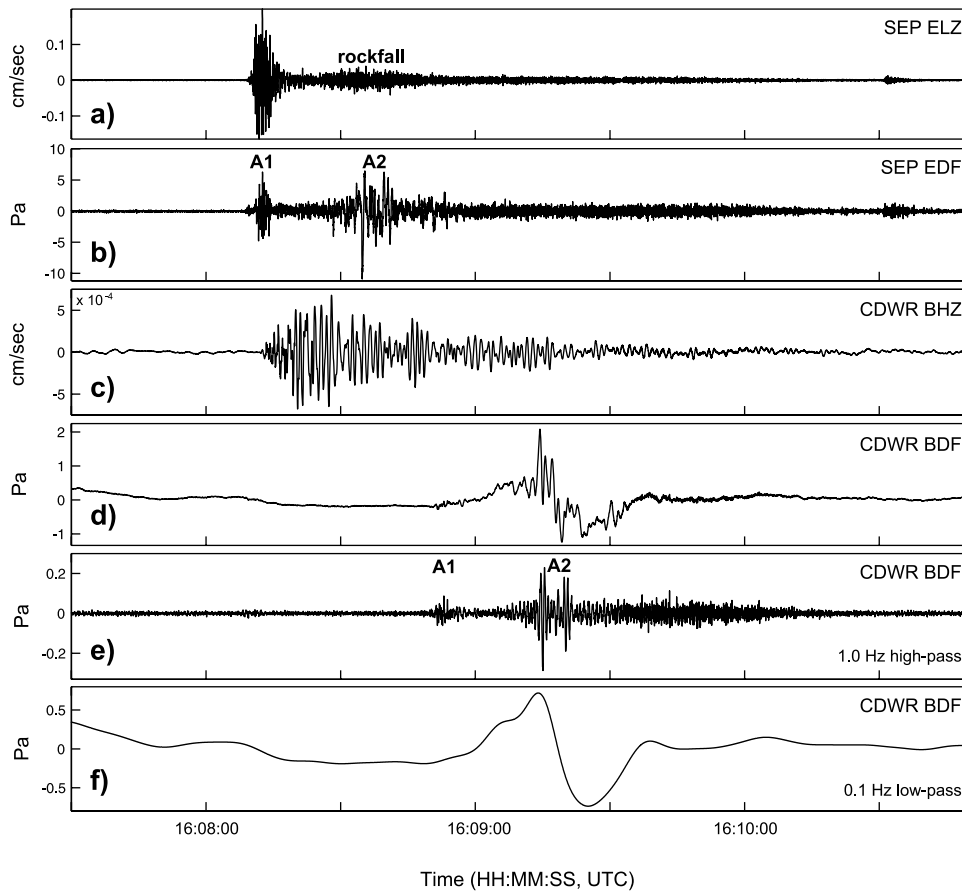


Figure 2. (a) Low-gain vertical-component record from station SEP. (b) Infrasonic signals recorded by a microphone at station SEP. A1 and A2 labels indicate timing of notable high-frequency infrasonic signals. (c) Broadband vertical-component record from station CDWR. (d) Unfiltered infrasonic signals recorded by a microphone at station CDWR. (e) Same as Figure 2d, but filtered with a 1.0 Hz high-pass filter. A1 and A2 labels indicate timing of notable high-frequency infrasonic signals. (f) Same as Figure 2d, but filtered with a 0.1 Hz low-pass filter.

2006 plume was initiated by a large rockfall, that no explosive activity was associated with this event, and that the associated steam plume originated from a location relatively far from the active vent. Thus some other process was responsible for generating the complex infrasonic signals and anomalously high plume.

4. Origin of VLP Infrasonic Signal

[10] Reported instances of VLP infrasonic signals are rare but not unprecedented. VLP pulses (~ 10 -s period) were recorded in association with several explosives-triggered snow avalanches in Wyoming, USA [Corney and Mendenhall, 2005], with the VLP signals arriving ~ 20 s after the explosion signal. A VLP pulse (~ 60 -s period) was recorded by an infrasonic sensor in Berkeley, California, during the climactic phase of the 18 May 1980 MSH eruption [Banister, 1984]. Acoustic gravity waves (tens-of-minutes period) were recorded by microbarographs in the Philippines in association with explosions leading up to the 14–15 June 1991 climactic eruption of Mount Pinatubo [Hoblitt *et al.*, 1996]. The 1980 MSH and Pinatubo signals featured an initial pressure increase followed by a pressure drop and

then a final pressure increase. Hoblitt *et al.* [1996] inferred that the initial pressure increase resulted from incorporation and expansion of air during formation of a fountain-fed pyroclastic surge, with the subsequent pressure decrease caused by air rushing in towards the surge after it had shed sufficient pyroclasts to rise vertically.

[11] Similar to the MSH and Pinatubo signals, the 29 May 2006 VLP pulse featured an initial pressure increase followed by a pressure decrease before returning to zero (Figure 2f). We attempted a waveform fit using an acoustic monopole source, relating the observed pressure waveform at 13.4 km to the flow of air mass in response to the rockfall [Lighthill, 2001]. A monopole approximation is valid when $ka \ll 1$, where $k = 2\pi/\lambda$ is the wavenumber, λ is the wavelength, and a is a characteristic dimension of the source, and far field radiation is defined by $kr \gg 1$, where r is the source-receiver distance. For the VLP signal, $\lambda \sim 17$ km (assuming a velocity of 340 m/s) and the length of the rockfall and mixed avalanche $a \sim 1.3$ km, hence $ka \sim 0.48$, while $r \sim 13.4$ km gives a kr of ~ 5 . Thus a monopole approximation is generally valid for the VLP signal. Linear-acoustic theory indicates that excess pressure



Figure 3. (a) Photograph from a remote camera located ~ 1 km east of vent (see Figure 1) taken 8 minutes after rockfall, showing southern half of MSH crater and steam plume (view is west–southwest). (b) Photograph taken one hour later from same location. (c) Photograph taken by W. E. Scott on 30 May 2006, showing entire rockfall deposit and most of the crater rim. Note that MSH crater is ~ 2 km wide. View is to south.

radiating from a monopole source in a half-space (assuming hemispherical spreading) is given by

$$p - p_0 = \frac{1}{2\pi r} \dot{q} \left(t - \frac{r}{c} \right) \quad (1)$$

where $p - p_0$ is the observed acoustic excess pressure, $\dot{q}(t)$ is the rate of change of the rate of mass outflow, and c is the speed of sound [Lighthill, 2001].

[12] To apply this model we formed a source-time function for mass outflow and inflow by inferring that outflow

was driven by rapid momentum transfer from the rockfall to the air and that inflow subsequently occurred to equalize pressure. We further inferred that inflow was slower than outflow, as inflow would have to overcome inertia of the surrounding air and would also possibly be temporarily blocked by momentum of outflowing air. Our mass-outflow function is shown in Figure 4c. The mass-outflow function has an air-outflow duration of 35 s, with subsequent inflow duration of 120 s. Although this model could certainly be refined, the synthetic acoustic pulse (Figure 4b) is a reasonable match to the observed VLP pulse (Figure 4a). Using the monopole model and assuming hemispherical spreading, we find that a total air mass of 7.5×10^6 kg is required to roughly match the observed VLP pulse at CDWR (Figure 4d). For an altitude of ~ 2 km (the vent height) and temperature of 0°C , the dry-air density is ~ 1.0 kg m^{-3} . This translates to a rockfall-displaced air-volume of 7.5×10^6 m^3 .

[13] The volume of displaced air can also be estimated using a simplified geometrical model of the rockfall and mixed avalanche. We use an equilateral triangle with 1.3 km-long base (the length of the rockfall) to represent the base area of the rockfall, and a triangular vertical cross-section tapering from 50 m height at the rockfall origin to zero at the northerly edge of the avalanche to represent the thickness. Such an object would displace an air volume of $\sim 10^7$ m^3 , roughly the same as the amount determined using the monopole model. The similarity between these two estimates indicates that air displaced by the rockfall and avalanche is a plausible explanation for the VLP signal.

5. Origin of A1 and A2 Infrasonic Signals

[14] The A1 and A2 infrasonic signals are too complex to model given large uncertainties in the source-time function of the rockfall-avalanche and atmospheric conditions. However, the delays between P -wave arrivals of the initial large-amplitude seismic signal and the A1 signal at SEP and CDWR are consistent with the expected difference for a sound wave generated at the time of the initial rockfall. Rockfalls of various sizes are a common occurrence in the crater and when witnessed, are always reported to be accompanied by appreciable acoustic noise. We infer that the initial infrasonic and seismic signals were created by large blocks cascading down the nearly vertical spine and landing at its base, a fall of ~ 50 – 100 m.

[15] The initial seismic signal at CDWR consists of P and R_g (Rayleigh wave) phases (the latter identified by its particle motions), indicating a shallow (< 3 km) source. To investigate whether the seismic signals could be generated by a falling mass rather than a “triggering” earthquake, we evaluated the velocity response to a falling-mass vertical force-time function [Stump, 1985] using the method of Kennett [1980] and the velocity model of Thelen *et al.* [2008]. Although this method does not account for topography, a force-time function with 1×10^7 N amplitude reproduces the 0.35 Hz R_g wave reasonably well, indicating that the observed seismic signals likely resulted from a falling mass rather than an earthquake.

[16] For the A2 pulse, the absence of a corresponding second seismic pulse indicates that A2 was not created by additional large blocks cascading down the spine, although a strong rockfall signal at SEP and CDWR at the time of A2

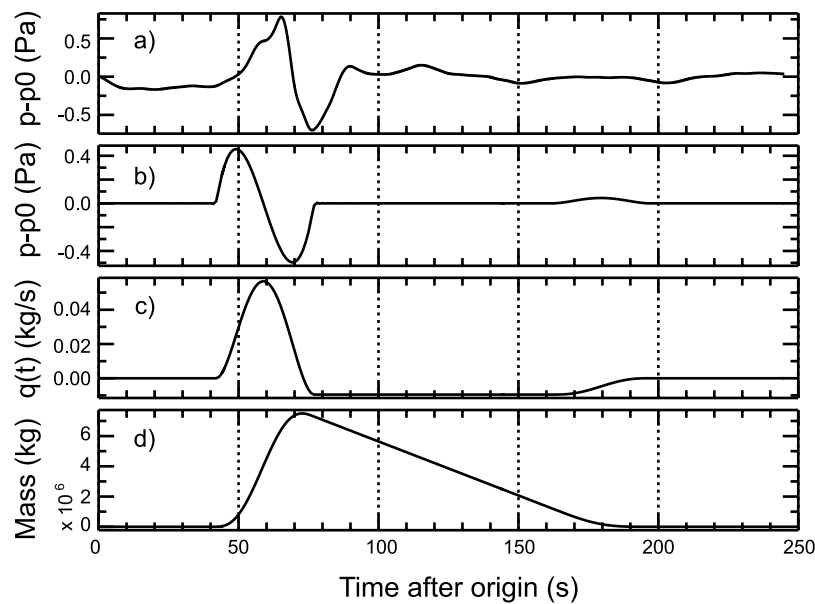


Figure 4. (a) Observed VLP infrasonic waveform recorded at CDWR. (b) Synthetic waveform derived from monopole model and mass outflow source-time function shown in Figure 4c. (c) Inferred source-time function for mass (air) outflow. (d) Modeled air-mass change over time.

indicates that the initial rockfall was still moving at that time (Figure 2a). The absence also indicates that A2 was not generated by collision of the rockfall against the base of the 1980–1986 lava dome, as such a collision would likely have coupled into the lava dome and produced a larger-amplitude seismic signal. Nevertheless, we infer that the A2 pulse was generated in the source area for the steam plume shown in Figure 3a. The 20 s lag time between the onsets of the A1 and A2 infrasonic signals is consistent with the time required for the rockfall to travel the 350 m from the source area to the depression, with the implied flow rate of ~ 17 m/s well within the bounds of measured rockfall velocities [e.g., Norris, 1994]. The evidence for snow scouring described above indicates that the rockfall was incorporating snow and ice as it moved across the snowfield. We infer that a significant fraction of the rockfall came to rest in the depression, with the entrained snow and ice coming into contact with hot dome rock and transforming to steam, creating the observed steam plume. However, we note that such a process would not have had sufficient thermal energy to produce the A2 infrasound pulse. Instead, we speculate that the A2 pulse was generated when air displaced by the rockfall (as described above in relation to the VLP signal) encountered the depression south of the 1980–1986 dome, producing short-duration infrasonic signals but not necessarily any ballistics.

6. Conclusions

[17] We analyzed seismic and infrasonic signals generated by a large rockfall and mixed avalanche at Mount St. Helens. We observed two high-frequency infrasonic signals (A1 and A2) superimposed over a Very Long-Period (VLP) signal. We found that synthetic waveforms produced by an acoustic monopole source model compared well to the observed signal, and on that basis infer that the VLP signal was caused by air displaced by the falling rock mass and

subsequent rockfall. Based on timing relations, we infer that the A1 infrasonic signal was caused by initial impact of the rockfall with the ground. Field relations indicate that the A2 pulse and observed steam plume were not caused by an explosion. Instead, we speculate that the A2 pulse was a result of air displaced by the rockfall encountering a depression at the base of the 1980–1986 lava dome.

[18] **Acknowledgments.** We thank Pat McChesney, Marvin Couchman, and Andy Lockhart for designing the SEP microphone/seismometer array and the Acoustic Surveillance for Hazardous Eruptions (ASHE) program for the CDWR data. Reviews by David Hill, Richard Iverson, and two anonymous reviewers are gratefully acknowledged. This work was partially supported by NSF grant EAR-0609669.

References

- Banister, J. R. (1984), Pressure wave generated by the Mount St. Helens eruption, *J. Geophys. Res.*, *89*, 4895–4904.
- Comey, R. H., and T. Mendenhall (2005), Recent studies using infrasound sensors to remotely monitor avalanche activity, in *ISSW 2004 Proceedings: A Merging of Theory and Practice*, edited by K. Elder, pp. 640–646.
- Dzurisin, D., J. W. Vallance, T. M. Gerlach, S. C. Moran, and S. D. Malone (2005), Mount St. Helens reawakens, *Eos Trans. AGU*, *86*, 25.
- Hoblitt, R. P., E. W. Wolfe, W. E. Scott, M. R. Couchman, J. S. Pallister, and D. Javier (1996), The preclimactic eruptions of Mount Pinatubo, June 1991, in *Fire and Mud: Eruptions and Lahars of Mount Pinatubo, Philippines*, edited by C. S. Newhall and S. Punongbayan, pp. 457–511, Univ. of Wash. Press, Seattle.
- Kennett, B. L. N. (1980), Seismic waves in a stratified half space - II. Theoretical seismograms, *Geophys. J. R. Astron. Soc.*, *61*, 1–10.
- Lighthill, J. (2001), *Waves in Fluids*, 2nd ed., 520 pp., Cambridge Univ. Press, Cambridge, U. K.
- Matoza, R. S., M. A. H. Hedlin, and M. A. Garcés (2007), An infrasound array study of Mount St. Helens, *J. Volcanol. Geotherm. Res.*, *160*, 249–262.
- McChesney, P. J., M. Couchman, S. C. Moran, A. B. Lockhart, K. J. Swinford, and R. G. LaHusen (2008), Seismic monitoring deployments and instrument development (seismic spider) at Mount St. Helens 2004–2005, in *A Volcano Rekindled: The Renewed Eruption of Mount St. Helens, 2004–2006*, edited by D. R. Sherrod, W. E. Scott, and P. H. Stauffer, *U.S. Geol. Surv. Prof. Pap.*, 1750, in press.
- Moran, S. C., P. J. McChesney, and A. B. Lockhart (2008), Seismicity and infrasound associated with explosions at Mount St. Helens, 2004–2005,

- in *A Volcano Rekindled: The Renewed Eruption of Mount St. Helens, 2004–2006*, edited by D. R. Sherrod, W. E. Scott, and P. H. Stauffer, *U.S. Geol. Surv. Prof. Pap.*, 1750, in press.
- Norris, R. D. (1994), Seismicity of rockfalls and avalanches at three Cascade Range volcanoes: Implications for seismic detection of hazardous mass movements, *Bull. Seismol. Soc. Am.*, 84, 1925–1939.
- Stump, B. W. (1985), Constraints on explosive sources with spall from near-source waveforms, *Bull. Seismol. Soc. Am.*, 75, 361–377.
- Thelen, W. A., R. S. Crosson, and K. C. Creager (2008), Absolute and relative locations of earthquakes at Mount St. Helens, Washington, using continuous data: Implications for magmatic processes, in *A Volcano Rekindled: The Renewed Eruption of Mount St. Helens, 2004–2006*, edited by D. R. Sherrod, W. E. Scott, and P. H. Stauffer, *U.S. Geol. Surv. Prof. Pap.*, 1750, in press.
- D. Bowers, AWE Blacknest, RG7 4RS Reading, UK.
- M. A. Garcés, Infrasound Laboratory, Hawai'i Institute of Geophysics and Planetology, University of Hawai'i at Manoa, Kailua-Kona, HI 96740-2638, USA.
- M. A. H. Hedlin and R. S. Matoza, Institute of Geophysics and Planetary Physics, Scripps Institution of Oceanography, University of California, San Diego, La Jolla, CA 92093-0225, USA.
- S. C. Moran, W. E. Scott, D. R. Sherrod, and J. W. Vallance, Cascades Volcano Survey, U.S. Geological Survey, Vancouver, WA 98683, USA. (smoran@usgs.gov)